Liquid chromatography/mass spectrometry

The HFM-treated samples were digested with sequencing grade-modified trypsin (Promega) and analyzed in duplicate using a nano-flow high-performance liquid chromatography (HPLC; NanoFrontier nLC, Hitachi High-technologies) connected to an electrospray ionization quadrupole time-of-flight (ESI-Q-TOF) mass spectrometer (Q-Tof Ultima, Waters).

MS peaks were detected, normalized, and quantified using the in-house 2DICAL software package, as described previously (17). A serial identification (ID) number was applied to each of the MS peaks detected (1 to 53,009). The stability of LC-MS was monitored by calculating the correlation coefficient (CC) and coefficient of variance (CV) of every measurement. The mean CC ± SD and CV ± SD for all 53,009 peaks observed in the 45 duplicate runs were as high as 0.946 ± 0.042 and as low as 0.053 ± 0.010, respectively.

Protein identification by tandem MS (MS/MS)

Peak lists were generated using the Mass Navigator software package (version 1.2; Mitsui Knowledge Industry) and searched against the SwissProt database (downloaded on April 22, 2009) using the Mascot software package (version 2.2.1; Matrix Science). The search parameters used were as follows. A database of human proteins was selected. Trypsin was designated as the enzyme, and up to 1 missed cleavage was allowed. Mass tolerances for precursor and fragment ions were ± 0.6 Da and ± 0.2 Da, respectively. The score threshold was set to $P < 0.05$ based on the size of the database used in the search. If a peptide was matched to multiple proteins, the protein name with the highest Mascot score was selected.

Western blot analysis

Primary antibodies used were a rabbit polyclonal antibody against platelet basic protein (PBP) precursor (Sigma) and a mouse monoclonal antibody against human complement C3b-α (PROGEN). The anti-PBP antibody recognizes all the known cleaved forms of PBP including CTAP-III and NAP-2. Six microliters of 1:10 diluted plasma sample was separated by SDS-PAGE and electroblotted onto a polyvinylidene difluoride (PVDF) membrane. The membrane was then incubated with the primary antibody and subsequently with the relevant horseradish peroxidase (HRP)-conjugated anti-rabbit or anti-mouse IgG, as described previously (26, 27). Blots were developed using an enhanced chemiluminescence (ECL) detection system (GE Healthcare).

Reverse-phase protein microarray

The plasma samples were passed through IgY microbeads (Seppro-IgY12, Sigma-Aldrich) using an automated Magtration System SA-1 (Precision System Science) in accordance with the manufacturer's instructions to reduce the 12 most abundant plasma proteins. The flow-through portion was serially diluted 1:50, 1:100, 1:200, and 1:400 using a Biomek 2000 Laboratory Automation Robot (Beckman Coulter) and randomly plotted onto ProteoChip glass slides (Proteogen) in quadruplicate in a 6,144-spot/slide format using a Protein Microarrayer Robot (Kaken Geneqs). The spotted slides were incubated overnight with the anti-PBP precursor antibody and then with biotinylated anti-rabbit IgG (Vector Laboratories) and subsequently with streptavidin-HRP conjugate (GE Healthcare). The peroxidase activity was detected using the Tyramide Signal Amplification (TSA) Cyanine 5 System (PerkinElmer). The slides were counterstained with Alexa Fluor 546-labeled goat anti-human IgG (Invitrogen; spotting control).

The stained slides were scanned on a microarray scanner (InnoScan 700AL; Innopsys). Fluorescence intensity, determined as the mean value of quadruplicate samples, was determined using the Mapix software package (Innopsys). All determined intensity values were transformed into logarithmic variables.

The reproducibility of the reverse-phase protein microarray assay was determined by repeating the same experiment, as reported previously (28). A plasma sample after reduction of the 12 most abundant plasma proteins was serially diluted within a range of 25- to 6,400-fold. Each diluted sample was spotted in quadruplicate onto glass slides and blotted with the anti-PBP antibody. In a representative quality control experiment, the CC value was 0.980 between days and the median CV was 0.047 among the quadruplicates.

Multiplex assay

The levels of CXCL7 in plasma samples were measured using a Milliplex Human Cytokine/Chemokine panel III kit (Millipore) in accordance with the manufacturer's instructions.

Statistical analysis

Statistical significance of intergroup differences was assessed with the Wilcoxon test, Mann–Whitney U test, Welch's t test, or Fisher's exact test, as appropriate. The area under the curve (AUC) of the receiver-operating characteristic (ROC) was calculated for each marker to evaluate its diagnostic significance. A composite index of 2 markers was generated using the results of multivariate logistic regression analysis, which also enabled the calculation of sensitivity, specificity, and the ROC curve. Statistical analyses were performed using an open-source statistical language R (version 2.7.0) with the optional module Design package.

Results

Plasma proteins associated with pancreatic cancer

A plasma sample from 1 healthy volunteer was processed 3 times using the HFM filtration technique. The concentration of β2-microglobulin before and after HFM treatment was measured. The recovery rates were
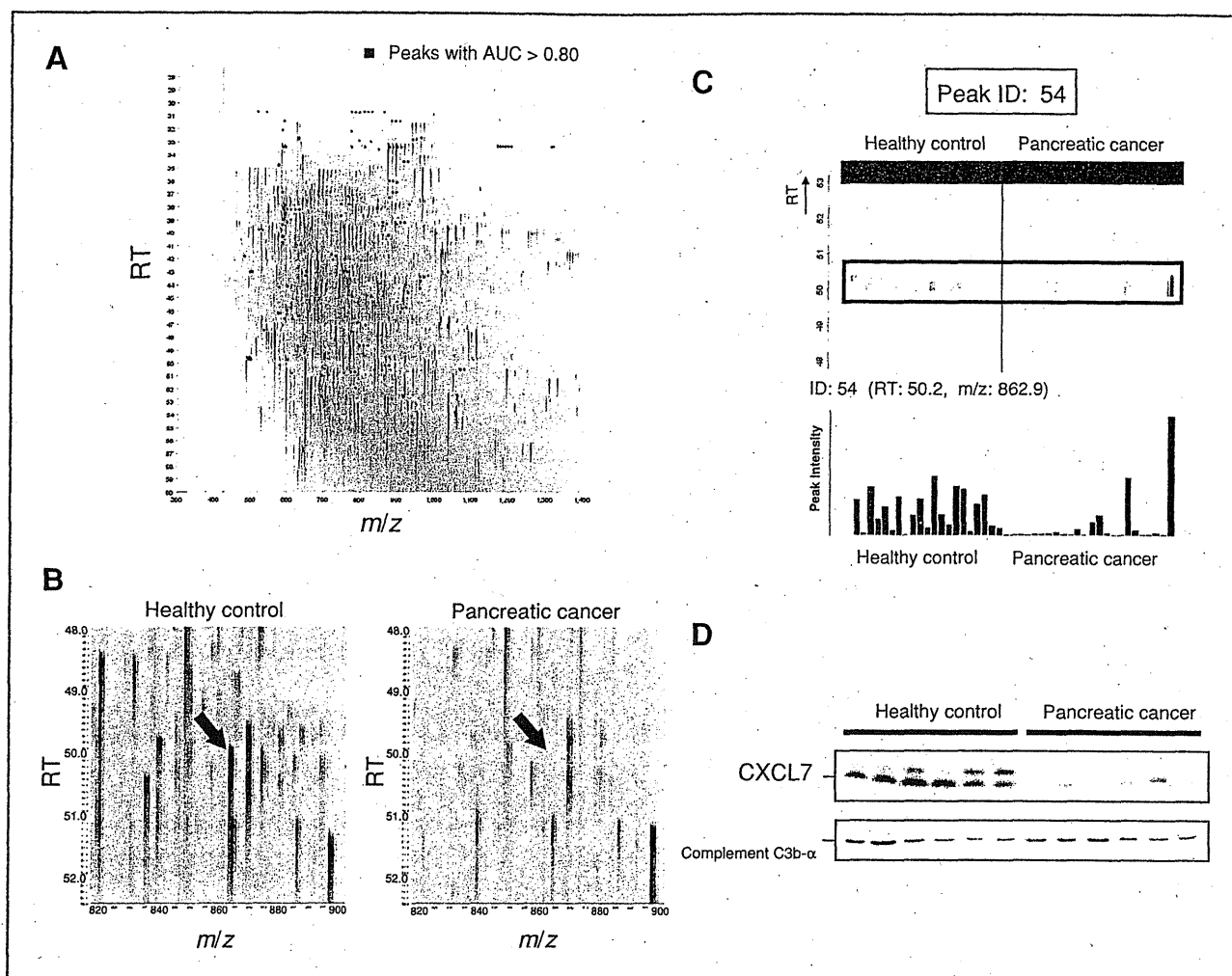
Figure 1. A, 2-dimensional display of all (>53,000) the MS peaks with m/z values along the x-axis and RT of LC along the y-axis. The peaks are displayed with a bin size of 1.0 m/z. The 140 MS peaks whose mean intensity of duplicates that distinguished pancreatic cancer patients from healthy controls with AUC values of greater than 0.800 are highlighted in red. B, CXCL7-derived MS peak (ID 54, at 863 m/z and 50.2 minutes) in representative patients from the cancer and control groups. C, CXCL7-derived MS peak (ID 54) in 45 duplicate LC-MS runs [patients with pancreatic cancer (red) and healthy controls (blue)] aligned along the RT of LC. Columns represent the mean intensity of duplicates (bottom). D, detection of CXCL7 and complement C3b-α (loading control) by Western blotting. Multiple bands for CXCL7 indicate the presence of proteolytic products.

25.11%, 25.73%, and 29.16%, respectively. Although the rates were seemingly low, the HFM treatment was highly reproducible with a CV of 0.081 and the amount of β2-microglobulin relative to total protein was increased 150 to 200-fold after HFM treatment.

To identify a diagnostic biomarker for pancreatic cancer, we compared the plasma LMW proteome between 24 patients with pancreatic cancer and 21 healthy controls (training cohort) using 2DICAL. Among a total of 53,009 independent MS peaks detected within the range 250 to 1,600 m/z and within a time range of 20 to 70 minutes, we found that 140 peaks had discriminatory ability with a AUC of above 0.800. Figure 1A is a representative 2-dimensional view of all the MS peaks displayed with m/z along the x-axis and the retention time (RT) of LC along the y-axis.

Twenty-five MS/MS spectra acquired from those 140 peaks were recurrently matched to 10 proteins in the database with a Mascot score of greater than 30 (Supplementary Table S1). Notably, one MS peak (ID 54) matched the amino acid sequence of the CXCL7 gene product (Swiss-Prot_P02775) with the highest score of 99.6 (Supplementary Fig. S2). Figure 1B shows the CXCL7-derived MS peak (ID 54, at 863 m/z and 50.2 minutes) that appeared in a representative pancreatic cancer patient and a healthy individual. Figure 1C demonstrates the distribution of the MS peak (ID 54) in patients with pancreatic cancer (red) and healthy controls (blue) in the training cohort (AUC = 0.839; $P = 4.54 \times 10^{-5}$; Mann–Whitney U test). The differential expression and identification of CXCL7 was confirmed by immunoblotting (Fig. 1D).

Validation of reduced CXCL7 in pancreatic cancer patients

The level of plasma CXCL7 was quantified in 12 patients with pancreatic cancer and 12 healthy individuals in the training cohort using multiplex assay. Consistent with 2DICAL, CXCL7 was found to be significantly decreased in patients with pancreatic cancer (mean ± SD, 744 ± 182 ng/mL) in comparison with healthy controls (1,355 ± 386 ng/mL; $P = 0.0003$). To further verify and validate the reduction of plasma CXCL7 in pancreatic cancer patients, 280 plasma samples [including 43 samples from the training cohort and new 237 samples (validation cohort)] were randomly plotted into a reverse-phase protein microarray and blotted with anti-PBP antibody (Fig. 2). Two samples from healthy controls in the training cohort were excluded due to an insufficient sample volume. Quadruplicate spots for representative cases and controls with high and low levels of CXCL7 are shown in the right panels of Figure 2.

The results of reverse-phase protein microarray were well correlated with those of multiplex assay (Pearson's $r = 0.65$; $P = 0.0006$; Supplementary Fig. S3). Microarray analysis also showed a significant reduction of the plasma CXCL7 level in the pancreatic cancer patients of the training cohort ($P = 5.96 \times 10^{-5}$; Welch's t test; Fig. 3A and Table 1) with an AUC value of 0.872 (95% CI: 0.732–0.951; Fig. 3B). The reduction of plasma CXCL7 was further validated in a larger independent cohort (validation cohort; $P = 1.40 \times 10^{-16}$; Fig. 3C and AUC value of 0.850, 95% CI: 0.792–0.895; Fig. 3B). Because there was a difference in age distribution between the cancer patients and healthy controls of the validation cohort (Table 1), we performed a subgroup analysis of 79 pancreatic cancer patients (median age, 61) and 20 healthy controls (median age, 60) aged 50 to 70 years. The reduction of plasma CXCL7 in patients with pancreatic cancer was statistically significant even in this subgroup ($P = 0.0001$), indicating that the decrease of the CXCL7 level was not merely due to the difference of age distribution between the pancreatic cancer patients and controls.

CXCL7 was significantly reduced in patients with any stage of pancreatic cancer (Table 2), including those with stage I (<0.001) and II (<0.001) disease. The significant alteration evident in early-stage patients indicated that the reduction of plasma CXCL7 is an early event in pancreatic carcinogenesis and may precede the development of cancer. The persistent presence of inflammation is known to promote carcinogenesis in various organs, and chronic pancreatitis is suspected to be one a precancerous condition for pancreatic cancer, although opinions on this issue vary. We measured the plasma level of CXCL7 in a small number of patients diagnosed as having chronic pancreatitis ($n = 10$) using the reverse-phase protein microarray (Table 1). The CXCL7 levels in patients with chronic pancreatitis were significantly lower than those in healthy controls ($P = 0.0002$), but slightly higher than those in patients with pancreatic cancer ($P = 0.095$; Fig. 3C).

Complementation of CA19-9 by CXCL7

CA19-9 is an established biomarker that has long been used for the diagnosis of pancreatic cancer. We found that the levels of CXCL7 and CA19-9 were not mutually correlated (Pearson's $r = 0.289$) and that combination with CXCL7 significantly improved the ability of CA19-9 to distinguish patients with pancreatic cancer from healthy controls: the AUC value improved to 0.965 (95% CI: 0.865–0.994) in the training cohort ($P = 0.026$) and to 0.961 (0.932–0.979) in the validation cohort ($P = 0.002$; Fig. 3D). The AUC values of CA19-9 in the 2 cohorts (Fig. 3D) were comparable with those reported previously (29–31).

Even among individuals with normal levels of CA19-9 (<37 U/mL; a cutoff value widely used in clinical practice), CXCL7 was significantly reduced in pancreatic cancer patients in both the training [$P = 0.014$ and AUC = 0.853 (95% CI: 0.650–0.957; Fig. 4A and B)] and validation [$P < 0.0001$ and AUC = 0.834 (95% CI: 0.747–0.899; Fig. 4B and C)] cohorts.

Because of the low prevalence of pancreatic cancer, any screening biomarker must have high specificity (32). The sensitivity/specificity of CA19-9 (cutoff: 37 U/mL) were 79%/89% in the training cohort and 79%/95% in the validation cohort, consistent with previous reports (32). If we defined the cutoff for CXCL7 as a level at which 95% of healthy individuals would be excluded, 83% of pancreatic cancer patients in the training cohort and 84% in the validation cohort would be detected using the combination of CXCL7 and CA19-9 (Supplementary Table S2).

Discussion

Early detection and subsequent radical surgical resection would most likely provide a chance of cure for patients with pancreatic cancer (7). However, patients with early-stage pancreatic cancer are generally asymptomatic and have little opportunity to undergo imaging and/or other diagnostic procedures until their disease becomes advanced. If a sensitive, but minimally invasive and cost-effective, plasma/serum test were available, it would be effective for alerting patients with early pancreatic cancer and offer them a chance to receive prompt and effective medical attention. In the present study, we compared the plasma LMW proteome between patients with pancreatic cancer and healthy controls using a new proteome platform, 2DICAL (Fig. 1), and found a significant decrease of the plasma CXCL7 level in patients with pancreatic cancer (Fig. 1B and C). The result of quantitative LC-MS was then verified using 3 different methods: immunoblotting (Fig. 1D), multiplex, and reverse-phase protein microarray (Figs. 2 and 3) assays. We further validated the significant decrease of CXCL7 in a larger independent cohort (validation cohort). The level of plasma CXCL7 was confirmed to be decreased reproducibly in patients with pancreatic cancer including those with Stage I and II disease (Table 2). CXCL7 did not
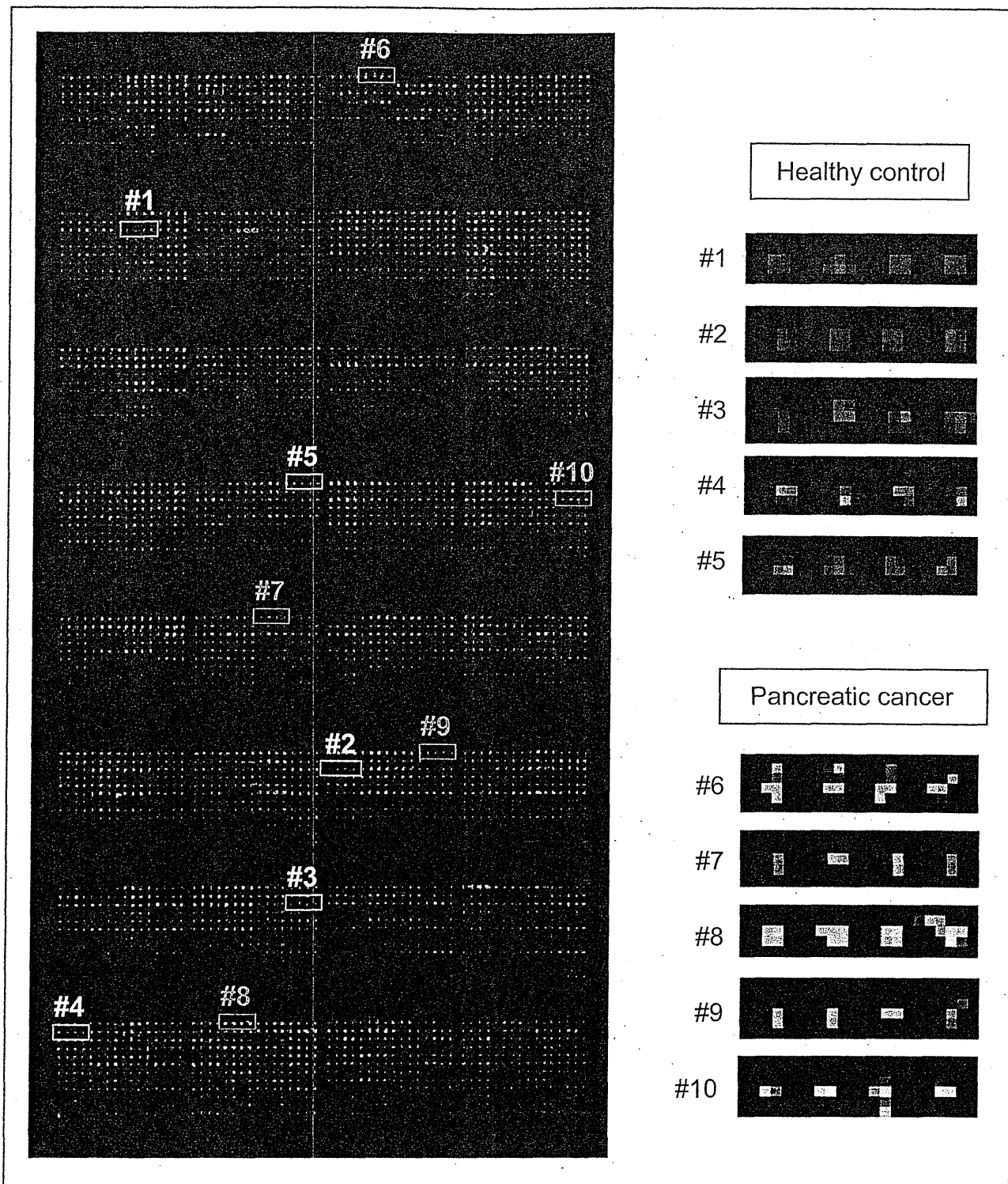
Figure 2. Image of a representative reverse-phase protein microarray slide stained with anti-PBP antibody (left). Samples were randomly assigned, and quadruplicate spots from representative patients with high and low levels of CXCL7 were extracted (right).

surpass the sensitivity of CA19-9, but was able to supplement it. Combination with CXCL7 significantly improved the sensitivity of CA19-9 (Fig. 3D and Supplementary Table S2).

In addition to 2DICAL, we utilized 2 state-of-the-art proteome technologies. The proteome analysis of plasma/serum samples has been hampered by the prominence of a handful of abundant proteins such as

Table 2. Plasma CXCL7 level according to clinical stage of pancreatic cancer

	Pancreatic cancer patients				Healthy controls
	Stage I	Stage II	Stage III	Stage IV	
Training cohort					
No. of cases	1	6	4	13	19[b]
CXCL7[a], mean (SD)	3.67 (-)	3.93 (0.24)	3.75 (0.17)	3.82 (0.33)	4.14 (0.18)
P (vs. healthy controls)	0.01	0.01	<0.001	<0.001	
Validation cohort					
No. of cases	5	25	40	70	87
CXCL7[a], mean (SD)	3.89 (0.34)	3.96 (0.25)	4.02 (0.18)	3.86 (0.32)	4.18 (0.14)
P (vs. healthy controls)	<0.001	<0.001	<0.001	<0.001	

NOTE. Welch's t test was applied to assess differences in values.
[a]Measured using reverse-phase protein microarrays.
[b]Two patients whose samples were not available for reverse-phase protein microarrays were excluded.

albumin and immunoglobulin. It is anticipated that the remaining proteins contain an unexplored archive of disease-driven information, but account for only about 1% of the entire human plasma proteome (24). To reduce the complexity of the plasma proteome, we used HFM filtration technology. Our HFM devise can separate and concentrate LMW plasma proteins in a fully automated manner (22) and allows identification of any biomarker candidate that is present at a level of 1 μg/mL. This discovery justifies the future application of the HFM system to more detailed proteome studies aimed at plasma/serum biomarker discovery. The other technology we employed is high-density reverse-phase protein microarray. The protein content of any human sample varies according to the individual, and therefore it is essential to distinguish biomarker candidates from simple interindividual heterogeneity. However, such distinction is possible only by comparing a statistically sufficient number of cases and controls. Our high-density protein microarrays require a minimal sample volume of the nanoliter order and make it possible to measure the quantity of any candidate biomarker protein in a statistically sufficient number of cases and controls (>300 samples; ref. 28) for judgment of its clinical potential in a single experiment.

LMW chemotactic cytokines have been implicated in various biological processes, such as leukocyte migration, angiogenesis, hematopoiesis, atherosclerosis, and cancer migration and metastasis. CXCL7, also known as PBP, is one of the members of the angiogenic ELR$^+$ CXC chemokine family (33). It is reportedly produced and stored in platelets, monocytes, neutrophils, and megakaryocytes. Secreted CXCL7 binds to CXC chemokine receptor 2 (CXCR2) on endothelium and mediates angiogenesis through activation of the Ras/Raf/mitogen-activated protein kinase (MAPK) and PI3K/AKT/mTOR signaling pathways (33, 34). The histology of pancreatic ductal

adenocarcinoma is often characterized by hypovascularization. The reduction of circulating CXCL7 in patients with pancreatic cancer may play a certain role in the suppression of angiogenesis.

Recently, reduction in the level of serum CXCL7 has been reported to be a biomarker for advanced myelodysplastic syndrome (35). In contrast, CXCL7 is increased in the pulmonary venous blood of lung cancer patients and is significantly decreased after curative surgical resection of the lung lesions. Of particular interest is the fact that the increment of CXCL7 is detectable several months before diagnosis of lung cancer (36). We observed a reduction of CXCL7 in 10 patients with chronic pancreatitis; but, examination of a larger number of patients will be needed before any definite conclusion can be reached.

CXCL7 is N-terminally truncated by cathepsin G-like enzymes and converted to other types of chemokines with distinct functions such as connective tissue-activating peptide III (CTAP-III) and neutrophil-activating peptide 2 (NAP-2; refs. 37, 38). One possible explanation for the reduction of plasma CXCL7 in patients with pancreatic cancer is degradation by certain exoproteases (39). Matrix metalloproteinase-9 (MMP9) has been reported to degrade CXC chemokines (40). MMP9 is often upregulated in pancreatic cancer cells and secreted into plasma (41). However, in this study, the precise molecular mechanisms behind the reduction of plasma CXCL7 in patients with pancreatic cancer remained unexplained.

Because the process of pancreatic carcinogenesis is probably mediated by various molecular pathways (42), the diagnosis of pancreatic cancer using a single biomarker may not be realistic, and a combination of different biomarkers with distinct spectra would appear to be a more realistic alternative. CA19-9 is the most widely used serum biomarker for pancreatic cancer; but, its sensitivity and specificity have been recognized
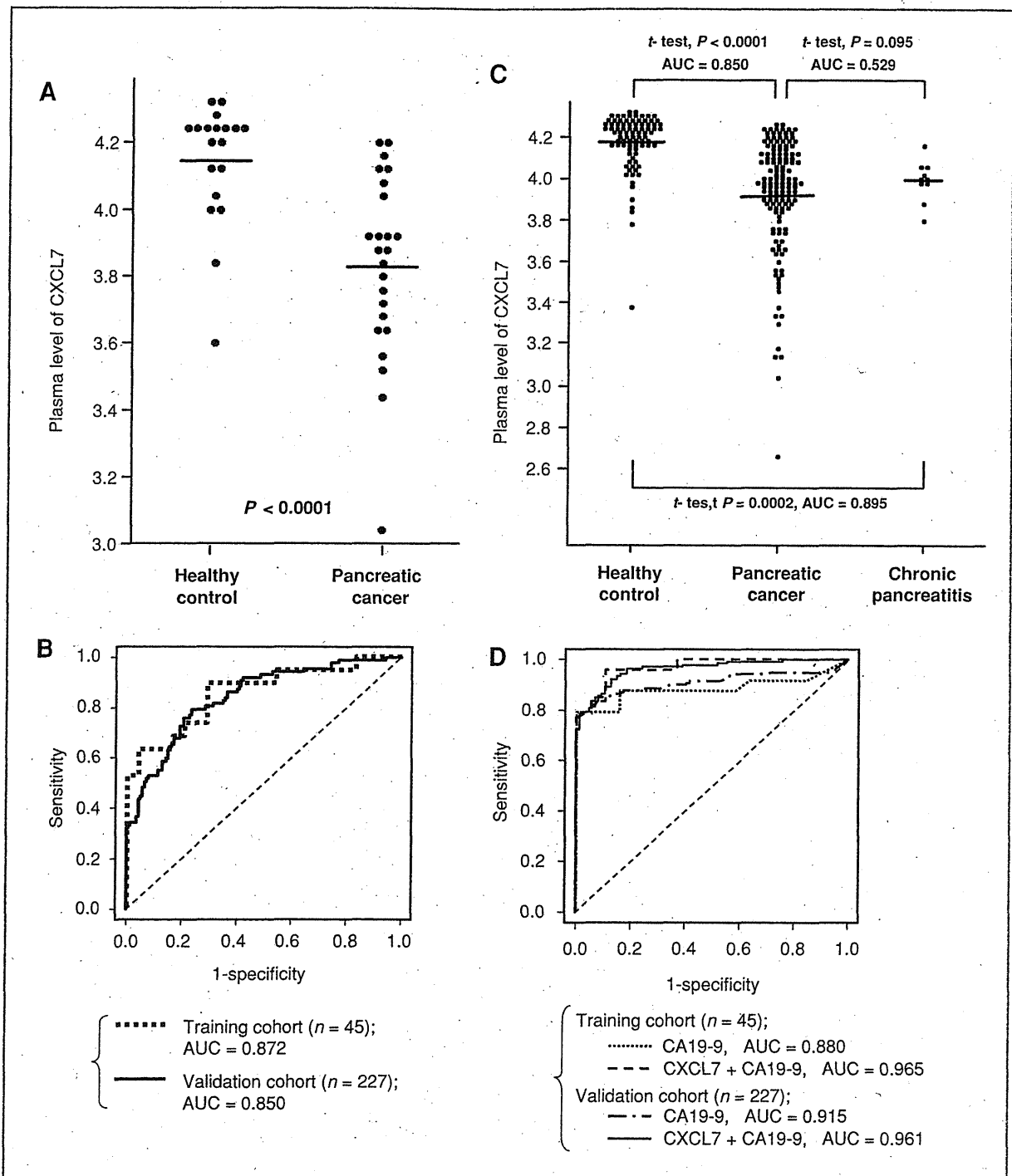
Figure 3. A and C, plasma levels (in arbitrary units) of CXCL7 in healthy controls, patients with pancreatic cancer, and patients with chronic pancreatitis in the training (A) and validation (C) cohorts. Horizontal lines represent the average levels of CXCL7. B, ROC analyses for the discriminatory value of CXCL7 in the training (dotted line) and validation (solid line) cohorts. D, ROC analyses for the discriminatory value of CA19-9 and the composite index of CA19-9 and CXCL7 in the training and validation cohorts.

to be unsatisfactory for pancreatic cancer screening (7, 12). We demonstrated that CXCL7 significantly improved the discriminatory ability of CA19-9, and this improvement was reproducibly validated in a large multi-institutional cohort. However, further independent validation by other investigators is still mandatory before its clinical application can be warranted (15, 29–31, 43).
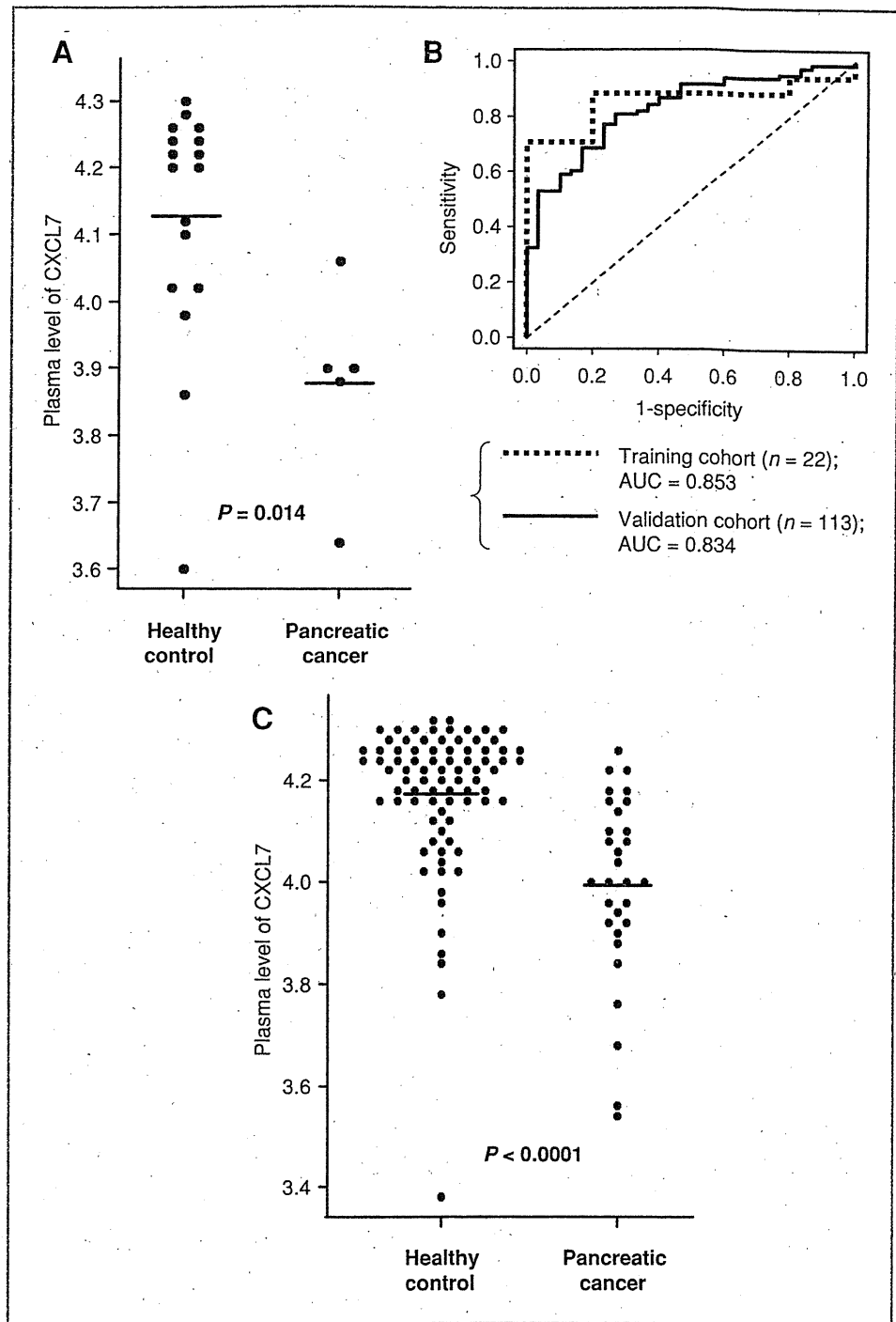
Figure 4. A and C, plasma levels of CXCL7 in healthy controls (left) and patients with pancreatic cancer (right) with the normal levels of CA19-9 (<37 U/mL) in the training (A) and validation (C) cohorts. Horizontal lines represent the average levels of CXCL7. B, ROC analyses of CXCL7 for discrimination between pancreatic cancer patients and healthy controls with normal levels of CA19-9 (<37 U/mL) in the training (dotted line) and validation (solid line) cohorts.

The primary goal of the present study was to discover new biomarkers useful for the early detection of pancreatic cancer in an asymptomatic population. Aberrations of circulating CXCL7 have also been reported in other premalignant conditions. The present study has not only explored the utility of CXCL7 as a biomarker, but also provided a novel insight into the chemokine-mediated reactions that occur during early carcinogenesis.

Disclosure of Potential Conflicts of Interest

Acknowledgment

Grant Support

References

1. Jemal A, Murray T, Samuels A, Ghafoor A, Ward E, Thun MJ. Cancer statistics, 2003. CA Cancer J Clin 2003;53:5–26.
2. Michl P, Pauls S, Gress TM. Evidence-based diagnosis and staging of pancreatic cancer. Best Pract Res Clin Gastroenterol 2006;20:227–51.
3. Ministry of Health, Labour and Welfare. Japanese Government: vital statistics of Japan2009. Available from: http://ganjoho.ncc.go.jp/professional/statistics/odjrh3000000hwsa-att/cancer_mortality(1958-2008).xls.
4. American Cancer Society. Cancer Facts and Figures2007. Atlanta, GA: American Cancer Society; 2007. p. 16–7.
5. Nitecki SS, Sarr MG, Colby TV, van Heerden JA. Long-term survival after resection for ductal adenocarcinoma of the pancreas. Is it really improving?Ann Surg 1995;221:59–66.
6. Tsuchiya R, Noda T, Harada N, Miyamoto T, Tomioka T, Yamamoto K, et al. Collective review of small carcinomas of the pancreas. Ann Surg 1986;203:77–81.
7. DiMagno EP, Reber HA, Tempero MA. AGA technical review on the epidemiology, diagnosis, and treatment of pancreatic ductal adenocarcinoma. American Gastroenterological Association. Gastroenterology 1999;117:1464–84.
8. Nieto J, Grossbard ML, Kozuch P. Metastatic pancreatic cancer 2008: is the glass less empty?Oncologist 2008;13:562–76.
9. Burris HA 3rd, Moore MJ, Andersen J, Green MR, Rothenberg ML, Modiano MR, et al. Improvements in survival and clinical benefit with gemcitabine as first-line therapy for patients with advanced pancreas cancer: a randomized trial. J Clin Oncol 1997;15: 2403–13.
10. Poplin E, Feng Y, Berlin J, Rothenberg ML, Hochster H, Mitchell E, et al. Phase III, randomized study of gemcitabine and oxaliplatin versus gemcitabine (fixed-dose rate infusion) compared with gemcitabine (30-minute infusion) in patients with pancreatic carcinoma E6201: a trial of the Eastern Cooperative Oncology Group. J Clin Oncol 2009;27:3778–85.
11. NCCN Clinical Practice Guidelines in Oncology: Pancreatic Adenocarcinoma V.1. National Comprehensive Cancer Network; 2009.
12. Goggins M. Molecular markers of early pancreatic cancer. J Clin Oncol 2005;23:4524–31.
13. Goggins M, Canto M, Hruban R. Can we screen high-risk individuals to detect early pancreatic carcinoma?J Surg Oncol 2000; 74:243–8.
14. Hanash S. Disease proteomics. Nature 2003;422:226–32.
15. Grantzdorffer I, Carl-McGrath S, Ebert MP, Rocken C. Proteomics of pancreatic cancer. Pancreas 2008;36:329–36.
16. Yamaguchi U, Nakayama R, Honda K, Ichikawa H, Hasegawa T, Shitashige M, et al. Distinct gene expression-defined classes of gastrointestinal stromal tumor. J Clin Oncol 2008;26:4100–8.
17. Ono M, Shitashige M, Honda K, Isobe T, Kuwabara H, Matsuzuki H, et al. Label-free quantitative proteomics using large peptide data sets generated by nanoflow liquid chromatography and mass spectrometry. Mol Cell Proteomics 2006;5:1338–47.
18. Matsubara J, Ono M, Negishi A, Ueno H, Okusaka T, Furuse J, et al. Identification of a predictive biomarker for hematologic toxicities of gemcitabine. J Clin Oncol 2009;27:2261–8.
19. Negishi A, Ono M, Handa Y, Kato H, Yamashita K, Honda K, et al. Large-scale quantitative clinical proteomics by label-free liquid chromatography and mass spectrometry. Cancer Sci 2009;100: 514–9.
20. Ono M, Matsubara J, Honda K, Sakuma T, Hashiguchi T, Nose H, et al. Prolyl 4-hydroxylation of alpha-fibrinogen: a novel protein modification revealed by plasma proteomics. J Biol Chem 2009;284:29041–9.
21. Anderson NL, Anderson NG. The human plasma proteome: history, character, and diagnostic prospects. Mol Cell Proteomics 2002; 1:845–67.
22. Tanaka Y, Akiyama H, Kuroda T, Jung G, Tanahashi K, Sugaya H, et al. A novel approach and protocol for discovering extremely low-abundance proteins in serum. Proteomics 2006;6:4845–55.
23. Kennedy S. The role of proteomics in toxicology: identification of biomarkers of toxicity by protein expression analysis. Biomarkers 2002;7:269–90.
24. Tirumalai RS, Chan KC, Prieto DA, Issaq HJ, Conrads TP, Veenstra TD. Characterization of the low molecular weight human serum proteome. Mol Cell Proteomics 2003;2:1096–103.
25. Available from: http://www.fhcrc.org/science/international_biomarker/.
26. Honda K, Yamada T, Hayashida Y, Idogawa M, Sato S, Hasegawa F, et al. Actinin-4 increases cell motility and promotes lymph node metastasis of colorectal cancer. Gastroenterology 2005;128:51–62.
27. Idogawa M, Yamada T, Honda K, Sato S, Imai K, Hirohashi S. Poly (ADP-ribose) polymerase-1 is a component of the oncogenic T-cell factor-4/beta-catenin complex. Gastroenterology 2005;128:1919–36.
28. Matsubara J, Ono M, Honda K, Negishi A, Ueno H, Okusaka T, et al. Survival prediction for pancreatic cancer patients receiving gemcitabine treatment. Mol Cell Proteomics 2010;9:695–704.
29. Fiedler GM, Leichtle AB, Kase J, Baumann S, Ceglarek U, Felix K, et al. Serum peptidome profiling revealed platelet factor 4 as a potential discriminating Peptide associated with pancreatic cancer. Clin Cancer Res 2009;15:3812–9.
30. Koopmann J, Zhang Z, White N, Rosenzweig J, Fedarko N, Jagannath S, et al. Serum diagnosis of pancreatic adenocarcinoma using surface-enhanced laser desorption and ionization mass spectrometry. Clin Cancer Res 2004;10:860–8.
31. Koopmann J, Buckhaults P, Brown DA, Zahurak ML, Sato N, Fukushima N, et al. Serum macrophage inhibitory cytokine 1 as a marker of pancreatic and other periampullary cancers. Clin Cancer Res 2004;10:2386–92.
32. Rhodes JM. Usefulness of novel tumour markers. Ann Oncol 1999;10Suppl 4:118–21.
33. Strieter RM, Burdick MD, Mestas J, Gomperts B, Keane MP, Belperio JA. Cancer CXC chemokine networks and tumour angiogenesis. Eur J Cancer 2006;42:768–78.
34. Heidemann J, Ogawa H, Dwinell MB, Rafiee P, Maaser C, Gockel HR, et al. Angiogenic effects of interleukin 8 (CXCL8) in human intestinal microvascular endothelial cells are mediated by CXCR2. J Biol Chem 2003;278:8508–15.
35. Aivado M, Spentzos D, Germing U, Alterovitz G, Meng XY, Grall F, et al. Serum proteome profiling detects myelodysplastic syndromes and identifies CXC chemokine ligands 4 and 7 as markers for advanced disease. Proc Natl Acad Sci USA 2007;104:1307–12.
36. Yee J, Sadar MD, Sin DD, Kuzyk M, Xing L, Kondra J, et al. Connective tissue-activating peptide III: a novel blood biomarker for early lung cancer detection. J Clin Oncol 2009;27:2787–92.
37. Ehlert JE, Ludwig A, Grimm TA, Lindner B, Flad HD, Brandt E. Down-regulation of neutrophil functions by the ELR(+) CXC chemokine platelet basic protein. Blood 2000;96:2965–72.
38. Pillai MM, Iwata M, Awaya N, Graf L, Torok-Storb B. Monocyte-derived CXCL7 peptides in the marrow microenvironment. Blood 2006;107:3520–6.

39. Villanueva J, Shaffer DR, Philip J, Chaparro CA, Erdjument-Bromage H, Olshen AB, et al. Differential exoprotease activities confer tumor-specific serum peptidome patterns. J Clin Invest 2006;116:271–84.

40. Van Den Steen PE, Proost P, Wuyts A, Van Damme J, Opdenakker G. Neutrophil gelatinase B potentiates interleukin-8 tenfold by aminoterminal processing, whereas it degrades CTAP-III, PF-4, and GRO-alpha and leaves RANTES and MCP-2 intact. Blood 2000;96:2673–81.

41. Tian M, Cui YZ, Song GH, Zong MJ, Zhou XY, Chen Y, et al. Proteomic analysis identifies MMP-9, DJ-1 and A1BG as overexpressed proteins in pancreatic juice from pancreatic ductal adenocarcinoma patients. BMC Cancer 2008;8:241.

42. Gansauge S, Gansauge F, Beger HG. Molecular oncology in pancreatic cancer. J Mol Med 1996;74:313–20.

43. Honda K, Hayashida Y, Umaki T, Okusaka T, Kosuge T, Kikuchi S, et al. Possible detection of pancreatic cancer by plasma protein profiling. Cancer Res 2005;65:10613–22.

Plasma biomarker discovery and validation for colorectal cancer by quantitative shotgun mass spectrometry and protein microarray

Yusuke Murakoshi,[1,2] Kazufumi Honda,[1] Shizuka Sasazuki,[3] Masaya Ono,[1] Ayako Negishi,[1] Junichi Matsubara,[1] Tomohiro Sakuma,[4] Hideya Kuwabara,[4] Shoji Nakamori,[5] Naohiro Sata,[6] Hideo Nagai,[6] Tatsuya Ioka,[7] Takuji Okusaka,[8] Tomoo Kosuge,[8] Masashi Shimahara,[9] Yohichi Yasunami,[10] Yoshinori Ino,[11] Akihiko Tsuchida,[2] Tatsuya Aoki,[2] Shoichiro Tsugane[3] and Tesshi Yamada[1,12]

[1]Chemotherapy Division, National Cancer Center Research Institute; [2]Third Department of Surgery, Tokyo Medical University; [3]Epidemiology and Prevention Division, Research Center for Cancer Prevention and Screening, National Cancer Center; [4]BioBusiness Group, Mitsui Knowledge Industry, Tokyo; [5]Department of Surgery, Osaka National Hospital, National Hospital Organization, Osaka; [6]Department of Surgery, Jichi Medical University, Tochigi; [7]Department of Hepatobiliary and Pancreatic Oncology, Osaka Medical Center for Cancer and Cardiovascular Diseases, Osaka; [8]Hepatobiliary and Pancreatic Oncology and Hepatobiliary and Pancreatic Surgery Divisions, National Cancer Center Hospital, Tokyo; [9]Department of Oral Surgery, Osaka Medical College, Osaka; [10]Department of Regenerative Medicine and Transplantation, Fukuoka University Faculty of Medicine, Fukuoka; [11]Pathology Division, National Cancer Center Research Institute, Tokyo, Japan

The development of a new plasma biomarker for early detection would be necessary to improve the overall outcome of colorectal cancer. Here we report the identification and validation of the ninth component of complement (C9) as a novel plasma biomarker for colorectal cancer by cutting-edge proteomic technologies. Plasma proteins were enzymatically digested into a large array of peptides, and the relative quantity of a total of 94 803 peptide peaks was compared between 31 colorectal cancer patients and 59 age/sex-matched healthy controls using 2D image-converted analysis of liquid chromatography and mass spectrometry. The selected biomarker candidates were validated in 345 subjects (115 colorectal cancer patients and 230 age/sex-matched healthy controls) using high-density reverse-phase protein microarrays. Plasma levels of Apo AI and C9 in colorectal cancer patients significantly differed from healthy controls with P values of 7.94×10^{-4} and 1.43×10^{-12} (Student's t-test), respectively. In particular, C9 was elevated in patients with colorectal cancer, including those with stage-I and -II diseases ($P = 3.01 \times 10^{-3}$ and $P = 1.13 \times 10^{-5}$, respectively). Although the significance of the present study must be validated in an independent clinical study, the increment of plasma C9 may be applicable to the early detection of colorectal cancer. (*Cancer Sci*, doi: 10.1111/j.1349-7006.2010.01818.x, 2010)

C olorectal cancer is the third most common cancer worldwide, with an estimated one and half million newly diagnosed cases every year.[1] In Japan, colorectal cancer is currently the third cause of cancer death in men and the first in women, but its incidence is predicted to increase and become the leading cause by 2015, most likely due to changing dietary habits as well as environmental conditions.[2,3] Successful prevention of death from colorectal cancer depends on its early detection. The surgical management of early stage colorectal cancer without metastasis is relatively uncomplicated. There is a significant level of evidence that the application of the fecal occult blood test to mass screening reduces the risk of colorectal cancer death, but its sensitivity and specificity, especially for early stage colorectal cancer, seem to be insufficient. Barium enema, flexible sigmoidoscopy/colonoscopy and ^{18}F-fluorodeoxyglucose positron emission tomography have higher specificity, but may not be cost- and labor-effective for mass screening of the asymptomatic general population.

The circulating blood proteome holds great promise as a reservoir of disease information, and a large variety of plasma/serum proteins have been used as disease biomarkers. Carcinoembryonic antigen (CEA) is a serum biomarker most widely used for colorectal cancer. However, the serum level of CEA often does not elevate in patients with colorectal cancer in the early stages and cannot be applicable to early detection of the disease.[4] We therefore have been searching for new serum/plasma biomarkers that can be used for mass survey of colorectal cancer.

Recently, various mass spectrometry (MS)-based proteomic technologies have been applied to clinical samples in the hope of identifying new disease biomarkers.[5–9] Among those technologies, shotgun proteomics has been considered the most promising because of its high sensitivity and protein identification capability: protein samples are enzymatically digested into a large array of peptides with uniform physical characteristics, and every peptide fragment is analyzed by liquid chromatography (LC) and MS. However, the number of samples that can be compared by shotgun proteomics is usually limited because isotope labeling is necessary to give a quantitative dimension to shotgun proteomics. The protein contents of each human sample vary significantly among individuals, and biomarker candidates can be distinguished from simple personal heterogeneity only by comparing a sufficient number of cases and controls. To overcome this limitation, we developed a software named 2D image converted analysis of liquid chromatography and MS (2DICAL),[9,10] which enabled accurate quantitative comparison across a theoretically unlimited number of LC-MS data without isotope labeling.[10] Using this powerful software we successfully identified biomarkers that can predict the hematological toxicities and survival of pancreatic cancer patients receiving gemcitabine.[11,12]

In the present study we searched for a biomarker that can be used for the early detection of colorectal cancer using 2DICAL. We carefully selected cases and controls to be compared by matching their age and gender distributions, as well as residential areas. We identified the significance increment of complement component C9 in the sera of patients with colorectal cancer, and its significance was validated in a large cohort using another innovative proteome technology, high-density reverse-phase protein microarray (RPPM).

---

[12]To whom correspondence should be addressed. E-mail: tyamada@ncc.go.jp

Materials and Methods

Patients and plasma samples. Plasma samples ($n = 345$) were collected from 115 patients diagnosed with colorectal cancer and 230 healthy volunteers matched with cancer patients by sex, age and residential area (two controls for each cancer patient; Table 1) between October 1998 and March 2002 with informed consent, as described previously.[13] Thirty-one cancer patients and 59 controls were randomly selected and subjected to 2DICAL analysis.

Another set of plasma samples were collected prospectively from 378 individuals including healthy volunteers and newcomers mainly to the Department of Gastroenterology at the National Cancer Center Hospital (Tokyo), Osaka National Hospital (Osaka), Jichi Medical School Hospital (Shimotsuke), Osaka Medical College (Osaka), Tokyo Medical University Hospital (Tokyo), Osaka Medical Center for Cancer and Cardiovascular Diseases (Osaka), and Fukuoka University Hospital (Fukuoka). This multi-institutional study was conducted as part of the "Third-Term Comprehensive Control Research for Cancer" conducted by the Ministry of Health, Labour and Welfare of Japan. Written informed consent was obtained from every individual, and the study protocol was approved by the ethics committee of each participating institution.

Sample preparation and LC-MS. Twelve abundant plasma proteins including albumin, IgG, $\alpha 1$-antitrypsin, IgA, IgM, transferrin, haptoglobin, $\alpha 1$-acid glycoprotein, $\alpha 2$-macroglobulin, Apo AI, apolipoprotein AII and fibrinogen were deduced from plasma samples using IgY-12 spin columns (Beckman Coulter, Fullerton, CA, USA) prior to MS analysis.[11] The deduced samples were precipitated with acetonitrile, dried and digested to peptide with modified trypsin. LC-MS and data acquisition were performed as described previously.[14] Briefly, MS spectra were acquired using nano-electrospray ionization (nano-ESI)-quadruple time-of-flight (QqTOF) MS (QTOF Ultima; Waters, Milford, MA, USA) every second for 60 min in the 250–1600 m/z range.

The MS peaks of each sample with the same m/z were extracted every 1 m/z and aligned. Peak lists were created using the Mass-Navigator software package (version 1.2; Mitsui Knowledge Industry, Tokyo, Japan). Targeted tandem MS (MS/MS) data were analyzed with the Mascot software package (version 2.2.1; Matrix Sciences, London, UK) against the NCBInr database (NCBInr_20070419. fast).

Antibodies. Anti-Apo AI rabbit polyclonal antibody was purchased from Calbiochem (Darmstadt, Germany), anti-C9 mouse monoclonal antibody from AntibodyShop (Gentofte, Denmark) and anti-$\alpha 2$-macroglobulin mouse monoclonal antibody from R&D Systems (Minneapolis, MN, USA).

Immunoblot analysis. Protein was separated by SDS-PAGE and transferred to polyvinyldene difluoride membrane, as described previously.[15] The membrane was incubated with anti-Apo AI, anti-C9 or anti-$\alpha 2$-macroglobulin (loading control) and then with relevant horseradish peroxidase (HRP)-conjugated secondary antibody. Blots were detected by ECL western blotting detection reagent according to the manufacturer's instruction (Amersham Biosciences, Buckinghamshire, UK).

RPPM. Plasma samples were serially diluted using PBS containing 0.01% triton X with or without 1% bovine serum albumin (BSA). The diluted plasma samples were printed onto slide glasses coated with ProLinker (ProteoChip; Proteogen, Seoul, Korea)[16,17] using a protein microarrayer equipped with 32 stainless steel pins of 100 µm diameter (Kakengeneqs, Matsudo, Japan) at 4°C. Printed microarray slides were incubated overnight at 37°C and stored at 4°C under desiccation. After returning to room temperature, the array slides were blocked with PBS containing 0.5% casein for 30 min and hybridized overnight with the first antibodies at 4°C. After washing, the array slides were hybridized with relevant biotinylated second antibodies (Vector Laboratories Inc. Burlingame, CA, USA) for 1 h and subsequently with avidin–HRP conjugated reagent (Amersham Biosciences) for 30 min. The fluorescent Cy5 signals were amplified using the tyramide signal amplification sys-

Table 1. Clinicopathological characteristics of individuals examined in the present study

	All cases ($n = 345$)			Cases analyzed by 2DICAL ($n = 90$)		
	Cancer ($n = 115$)	Healthy ($n = 230$)	P value	Cancer ($n = 31$)	Healthy ($n = 59$)	P value
Age (mean ± SD) (years)	59.3 ± 8.9	59.4 ± 8.9	0.93‡	56.8 ± 9.9	56.4 ± 9.8	0.79‡
Gender						
Male	71	142	0.92§	20	36	0.75§
Female	44	88		11	23	
Primary site						
Cecum	6			0		
Ascending colon	27			9		
Transverse colon	8			4		
Descending colon	5			3		
Sigmoid colon	18			5		
Rectum	51			10		
Clinical stage†						
0	17			5		
I	35			10		
II	28			7		
III	25			6		
IV	10			3		
Histology						
Well-differentiated adenocarcinoma	74			21		
Moderately differentiated adenocarcinoma	37			8		
Poorly differentiated adenocarcinoma	2			1		
Others	2			1		

†According to TNM Classification of Malignant Tumors (International Union Against Cancer), 6th Edition. ‡Student's t-test. §Chi-square test.
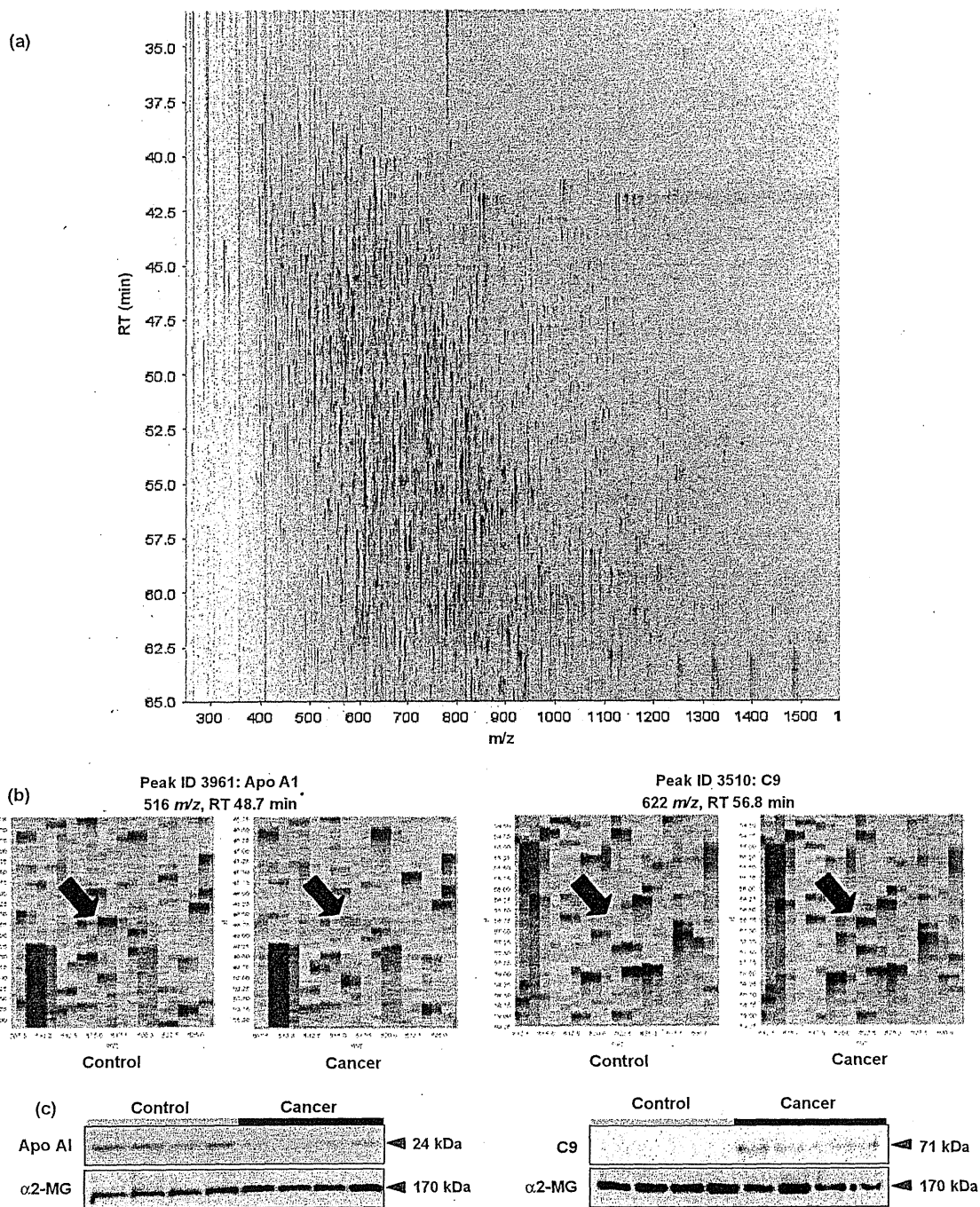
Fig. 1. Plasma biomarker discovery by 2D image converted analysis of liquid chromatography and mass spectrometry (2DICAL). (a) Two-dimensional display of >90 000 peaks of a representative sample with retention time (RT; in minutes) along the vertical (X) axis and with mass to charge (m/z) ration value along the horizontal (Y) axis. (b) Peptide peaks derived from apolipoprotein AI (Apo AI; left; ID 3961) and complement component C9 (C9; right; ID 3510) in a representative colorectal cancer patient (Cancer) and a representative healthy individual (Control). (c) Detection of Apo AI, C9 and α2-macroglobulin (α2-MG, loading control) in plasma samples of four representative colorectal cancer patients and four healthy controls by immunoblotting.

tem (Perkin Elmer, Boston, MA, USA) according to the manufacturer's instructions. Counterstaining was performed with Alexa 488-labeled anti-human IgG antibody (Invitrogen, Carlsbad, CA, USA). Dual-color fluorescent signals (green and red) were detected with a confocal laser microarray scanner (Inno-Scan 700 AL; Innopsys, Carbonne, France). The median signal intensity of quadruplicates was calculated using the Mapix software (Innopsys).

Measurement of CEA. The plasma level of CEA was determined using the CEA Enzyme Immunoassay kit (Hope Laboratories, Belmont, CA, USA) according to the manufacturer's instruction.

Statistical analysis. Statistically significant differences were detected using Paired t-test and Student's t-test. Interquartile range (IQR), receiver operator characteristics (ROC) and area under the curve (AUC) analyses were performed using the

Table 2. Protein identification of peptide peaks with significant difference between colorectal cancer patients and healthy controls

ID	M/Z	RT	prot_acc	prot_desc	Cancer†	Control†	pep_score	AUC	P-value‡	pep_seq
664	651.33	46.18	APOA1_HUMAN	Apolipoprotein A-I precursor (Apo-AI) (ApoA-I) (contains: apolipoprotein A-I [1-242])	34.01 ± 18.34	60.26 ± 41.89	58.87	0.77	0.00038	THLAPYSDELR
3961	516.78	48.71	APOA1_HUMAN	Apolipoprotein A-I precursor (Apo-AI) (ApoA-I) (contains: apolipoprotein A-I [1-242])	11.40 ± 3.85	17.32 ± 7.43	49.08	0.81	0.00006	LSPLGEEMR
2384	632.03	63.40	A2GL_HUMAN	Leucine-rich alpha-2-glycoprotein precursor (LRG)	42.66 ± 23.89	24.61 ± 10.75	46.04	0.79	0.00094	ENQLEVLEVSWLHGLK
2819	506.81	45.11	APOA1_HUMAN	Apolipoprotein A-I precursor (Apo-AI) (ApoA-I) (contains: apolipoprotein A-I [1-242])	16.56 ± 7.20	26.31 ± 14.57	45.5	0.77	0.00063	AKPALEDLR
516	642.31	52.07	APOA1_HUMAN	Apolipoprotein A-I precursor (Apo-AI) (ApoA-I) (contains: apolipoprotein A-I [1-242])	41.38 ± 21.38	79.15 ± 64.65	33.51	0.76	0.00040	WQEEMELYR
5489	728.37	57.22	CO9_HUMAN	Complement component C9 precursor (contains: complement component C9a; complement component C9b)	22.00 ± 8.48	15.71 ± 4.73	32.3	0.75	0.00000	AIEDYINEFSVR
3510	621.88	56.75	CO9_HUMAN	Complement component C9 precursor (contains: complement component C9a; complement component C9b)	34.36 ± 18.88	18.48 ± 8.90	26.47	0.77	0.00003	LSPIYNLVPVK
3401	618.36	59.06	APOA1_HUMAN	Apolipoprotein A-I precursor (Apo-AI) (ApoA-I) (contains: apolipoprotein A-I [1-242])	15.13 ± 4.59	25.00 ± 13.78	25.32	0.77	0.00022	DLATVYVDVLK
393	626.82	50.77	APOA1_HUMAN	Apolipoprotein A-I precursor (Apo-AI) (ApoA-I) (contains: apolipoprotein A-I [1-242])	45.28 ± 25.93	88.60 ± 65.21	25.1	0.79	0.00005	VQPYLDDFQK
3615	743.04	48.25	STX16_HUMAN	Syntaxin-16 (Syn16)	16.95 ± 14.15	9.81 ± 3.18	24.74	0.75	0.02199	RPPPKWVDGVDEIQYDVGR
348	615.86	61.43	APOA1_HUMAN	Apolipoprotein A-I precursor (Apo-AI) (ApoA-I) (contains: apolipoprotein A-I [1-242])	55.73 ± 34.80	109.93 ± 75.99	23.96	0.77	0.00008	QGLLPVLESFK
5664	622.33	57.48	PDGFD_HUMAN	Platelet-derived growth factor D precursor (PDGF D)	25.96 ± 9.12	21.18 ± 7.81	21.52	0.66	0.00001	LIFVYTLICANFCSCR
11415	1057.01	48.26	EP400_HUMAN	E1A-binding protein p400 (EC 3.6.1.-) (p400 kDa SWI2/SNF2-related protein)	11.57 ± 4.37	8.79 ± 2.29	18.02	0.75	0.01037	GRPPIATFSANPEAKAAAAPFQTSQASASAPR
2259	941.45	60.01	KCD10_HUMAN	BTB/POZ domain-containing protein KCTD10	71.39 ± 18.04	61.47 ± 17.33	16.49	0.66	0.00010	EEMSGESVVSSAVPAAATR
6778	804.81	46.45	DIP2A_HUMAN	Disco-interacting protein 2 homolog A	10.73 ± 5.51	7.57 ± 1.59	16.21	0.77	0.00017	KAVLSMNGLSYGVIR
7297	804.98	46.47	K0460_HUMAN	Uncharacterized protein KIAA0460	9.99 ± 5.47	6.87 ± 1.49	16.02	0.78	0.00005	AAGGGGGSSKASSSSASSAGALESSLDR
7749	662.33	46.17	ADPPT_HUMAN	L-Aminoadipate-semialdehyde dehydrogenase-phosphopantetheinyl transferase (EC 2.7.8.-)	10.70 ± 2.16	14.59 ± 5.05	15.92	0.77	0.00206	FTNKEWETIR

†Data are presented as mean ± SD. ‡Paired t-test. AUC, area under curve; RT, retention time.

components available in R-project (http://www.r-project. org/).[11] A composite index of two markers was generated using the results of multivariate logistic regression analysis, which also enabled calculation of the ROC curve.

Results

Identification of biomarker candidates. We compared plasma proteome data between 31 colorectal cancer patients and 59 healthy volunteers (Table 1) using 2DICAL. A total of 94 803 independent peptide peaks were detected across the 90 cases (Fig. 1a) and numbered from ID1 to ID94803. Ninety MS peaks showed a statistically significant difference between healthy controls and colorectal cancer patients (maximum mass peak intensity > 10 [arbitrary unit] and $P \leq 0.0001$ [Paired t-test] or AUC ≥ 0.75). Twenty-nine peaks were further selected by visual inspection (Fig. 1b) and subjected to MS/MS analysis. MS/MS spectra obtained from 17 peptide peaks matched 10 proteins deposited in the NCBInr database (Table 2). We selected two proteins, Apo AI and C9, for further analyses because the same protein annotation was obtained from at least two independent peaks.

Identification and differential expression of Apo AI and C9 were confirmed by immunoblotting plasma samples of representative cases (Fig. 1c). Apo AI was downregulated in cancer patients, while C9 was upregulated.

Establishment of RPPM. For the rapid selection and validation of plasma biomarker candidates, we established a high-density protein microarray platform. Plasma samples were serially diluted and printed in quadruplicate onto a hydrophobic glass surface in a format of 6144 spots within an area of 17.65 × 34.57 mm. The location of each spot was visualized by staining human IgG (green), and the relative amounts of Apo AI and C9 proteins were quantified by hybridization with antibodies (red). Fluorescent signal intensity showed linearity in the plasma dilution range of ×32 to ×4096 in a quality control experiment (Fig. 2a) and was highly reproducible among four independent experiments (Fig. 2b). Over 78% of spots showed coefficients of variation (CV) values of < 0.1 (Fig. 2c).

Validation of biomarker candidates. In order to examine the significance of Apo AI and C9 in a larger cohort, we used RPPM, onto which plasma samples were spotted in a high-density manner. The plasma samples were serially diluted and randomly printed four times onto a microarray. Figure 3a depicts the entire image of RPPM stained with anti-C9 antibody. Representative blots of colorectal cancer and control samples are shown in Figure 3b. The RPPM revealed that Apo AI was downregulated in colorectal cancer patients compared with healthy controls, and the difference between colorectal cancer and healthy controls was statistically significant ($P = 0.000794$; Fig. 3c). C9 was significantly upregulated in colorectal cancer ($P = 1.43 \times 10^{-12}$; Fig. 3d). The results of RPPM were well correlated with those of immunoblot assay (Fig. S1), thus confirming the preciseness of RPPM.

The AUC values of Apo AI and C9 were 0.621 and 0.730, respectively (Fig. 3e,f). Although the level of plasma Apo AI was significantly different between colorectal cancer patients and healthy controls, the utility of Apo AI as a biomarker of colorectal cancer seems to be limited due to its relatively low AUC value. Statistically significant differences for upregulation of C9 were observed in patients with stage I, II, III and IV[18] colorectal cancer ($P = 3.02 \times 10^{-3}$, 1.13×10^{-5}, 5.22×10^{-8} and 3.45×10^{-4}, respectively; Fig. 3g). The AUC values of C9 for the early (stages 0–II) and advanced (stages III and IV) colorectal cancer patients were 0.667 and 0.862, respectively.
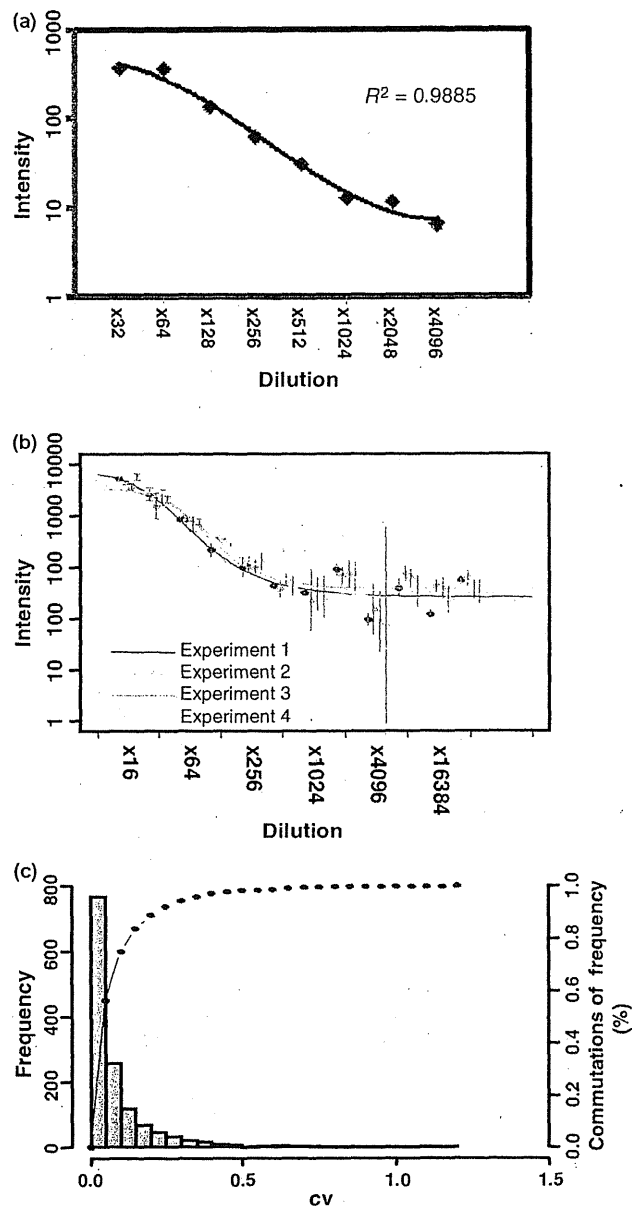

Fig. 2. Reproducibility of reverse-phase plasma microarray (RPPM). (a) Linearity of RPPM. A plasma sample was serially diluted from 32 to 4096 folds and spotted onto a ProteoChip glass. The glass was stained with anti-apolipoprotein AI antibody as described in the Materials and Methods. The mean fluorescence intensity of quadruplicates (vertical axis in arbitrary units) is plotted against plasma dilution (horizontal axis). (b) Reproducibility of RPPM. A plasma sample was serially diluted from 16 to 32 768 folds and processed as described above. The same experiment was conducted four times (Experiments 1–4), and their dilution curves overlapped. The dots represent the median intensity of quadruplicates. Bars represent interquartile ranges (IQR). (c) Distribution of the coefficients of variation (CV) values among quadruplicates in the 6144 spots (1536 quadruplicates) of RPPM stained with anti-Apo AI antibody. The dotted line represents cumulative frequency (%; right vertical axis label).

We measured the plasma level of CEA in 42 samples (20 healthy controls and 22 colorectal cancer patients: stage 0 [$n = 2$], stage I [$n = 5$], stage II [$n = 5$], stage III [$n = 5$] and stage IV [$n = 5$]), for which the residual sample volume was sufficient for the measurement with enzyme-linked immunosorbent assay (ELISA). The AUC values of CEA for the early
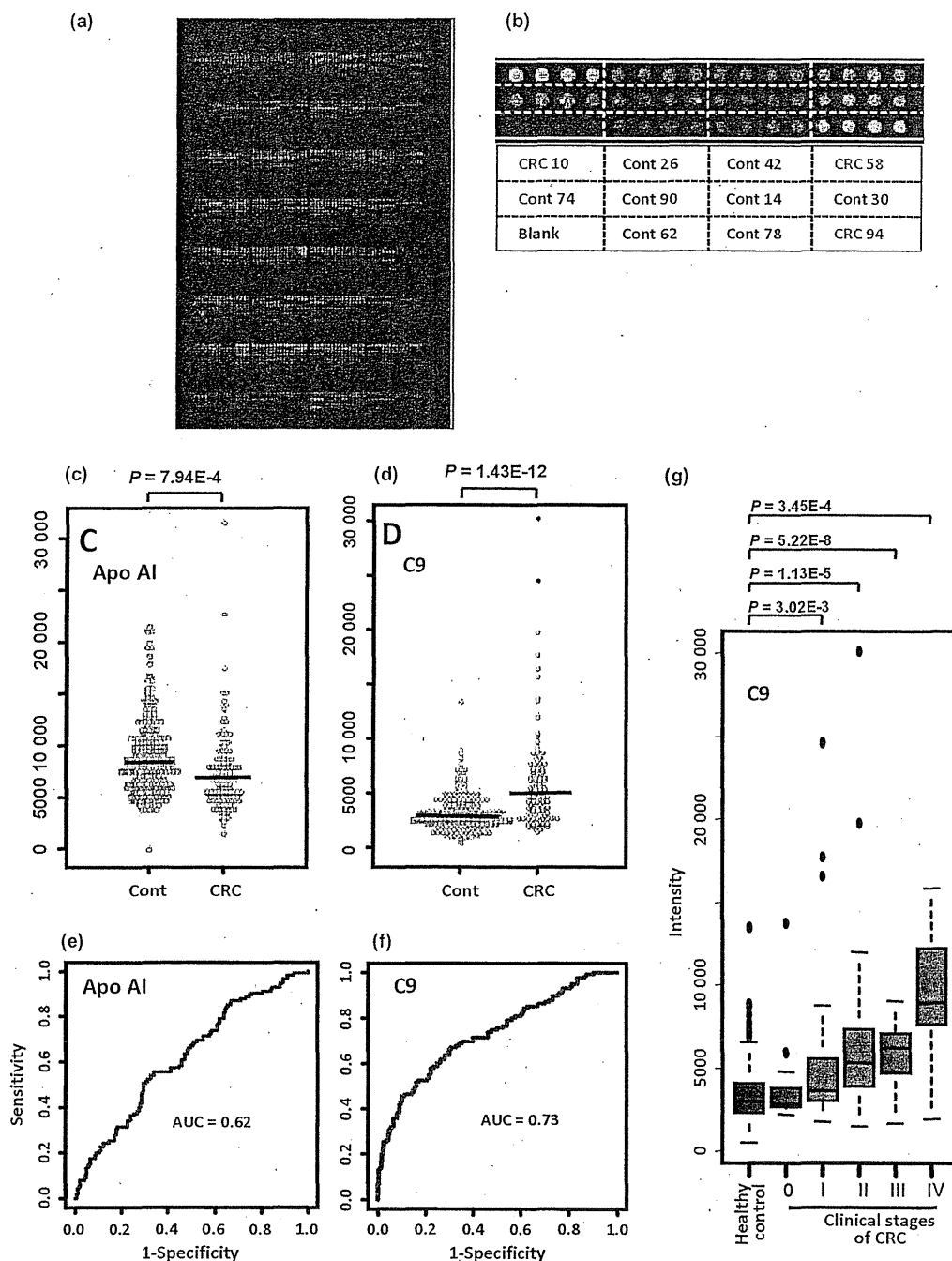
Murakoshi et al.

(a)

(b)

CRC 10	Cont 26	Cont 42	CRC 58
Cont 74	Cont 90	Cont 14	Cont 30
Blank	Cont 62	Cont 78	CRC 94

(c) $P = 7.94E-4$

C
Apo AI

Cont   CRC

(d) $P = 1.43E-12$

D
C9

Cont   CRC

(g)

$P = 3.45E-4$
$P = 5.22E-8$
$P = 1.13E-5$
$P = 3.02E-3$

C9

Intensity

Healthy control   0   I   II   III   IV

Clinical stages of CRC

(e)

Apo AI

Sensitivity

AUC = 0.62

0.0   0.2   0.4   0.6   0.8   1.0
1-Specificity

(f)

C9

AUC = 0.73

0.0   0.2   0.4   0.6   0.8   1.0
1-Specificity

Fig. 3. Validation of altered plasma apolipoprotein AI (Apo AI) and C9 in colorectal cancer by reverse-phase plasma microarray (RPPM). (a) Dual-color scanning image of RPPM, on which serially (64- to 512-fold) diluted plasma samples of colorectal cancer patients (n = 115) and healthy controls (n = 230) were randomly spotted in quadruplicate. The RPPM was stained with anti-complement component C9 (red) and anti-human IgG (green) antibodies, as described in the Materials and Methods. (b) Representative spots of colorectal cancer patients (CRC) and healthy controls (Cont). (c) Distribution and median values (vertical bars) of the plasma Apo AI level (in arbitrary units) measured by RPPM. A statistically significant difference was recognized between healthy controls and colorectal patients (P = 0.00794, Student's t-test). (d) Distribution and median values (vertical bars) of plasma C9 level (in arbitrary units) measured by RPPM. Statistical significance was recognized between healthy controls and colorectal patients (P = 1.43 × 10^{-12}, Student's t-test). (e) Receiver operator characteristic (ROC) analysis of Apo AI. AUC, area under the curve. (f) ROC analysis of C9. (g) Box-and-whisker diagram showing the different plasma levels of C9, determined by RPPM for healthy controls and each clinical stage of colorectal cancer. Boxes represent the median values and the 25–75 percentile ranges. Whiskers indicate the most extreme data point, which are no more than 1.5 times the interquartile ranges from the boxes.

(stages 0–II) and advanced (stages III and IV) colorectal cancer patients over healthy individuals were 0.594 and 0.810, respectively, indicating its inferiority to C9 in detecting early stage colorectal cancer.

Alterations of Apo AI and C9 in other cancers. Finally, we measured the level of Apo AI and C9 in 378 plasma samples collected prospectively from different medical institutions using RPPM. The observed alterations of plasma Apo AI and C9

6

Table 3. Alterations of plasma Apo AI and C9 in various diseases

	n	Apo AI			C9		
		Average†	SD	P value‡	Average†	SD	P value‡
Healthy control	109	4679.5	3265.6		527.2	674.7	
Colorectal cancer	100	2318.4	2015.0	1.71×10^{-9}	1792.7	1628.1	3.82×10^{-11}
Gastric cancer	105	2812.0	2357.5	3.00×10^{-6}	1629.6	1533.9	3.31×10^{-10}
Hepatocellular carcinoma	14	2621.6	2260.8	0.007	477.0	332.4	0.651
Esophageal cancer	10	3074.6	1572.6	0.014	1639.1	1036.7	0.008
Pancreatic cancer	14	2934.3	2214.8	0.016	1436.8	1125.6	0.010
Cholangiocarcinoma	18	1674.6,	1377.0	1.26×10^{-8}	2519.6	2086.8	0.001
Pancreatitis	8	1925.9	1970.3	0.005	1564.4	1502.5	0.093

†Determined by RPPM (in arbitrary units). ‡Compared with healthy controls (student's t-test).

proteins in colorectal cancer patients were reproducible, even in this independent cohort (Table 3). The reduction of plasma Apo AI protein seems not to be specific to colorectal cancer, and was observed in patients with various cancers as well as chronic pancreatitis. The increment of plasma C9 protein was also not specific to colorectal cancer patients; patients with gastric cancer, esophageal cancer, pancreatic cancer and cholangiocarcinoma also showed a statistically significant increase of plasma C9 protein. The AUC value of C9 for colorectal cancer patients over healthy individuals (0.796) was higher than that of CEA (0.762; Fig. 4). The combination with C9 improved the AUC value of CEA from 0.762 to 0.852.

Discussion

The context of circulating blood proteins may represent underlying physiological and pathogenic conditions. Therefore, the blood proteome is considered an ample source of biomarker discovery. In order to identify a new biomarker that can be used for a non-invasive and inexpensive blood test of colorectal cancer, we first compared plasma proteome data using 2DICAL. We found that 10 proteins showed statistically significant differences between colorectal cancer patients and controls (Table 2). The differences of Apo AI and C9 were then verified by immunoblotting with relevant antibodies (Fig. 1c). Apo AI is the major protein component of plasma high density lipoprotein.[19] Apo AI has been repeatedly reported to be downregulated in the plasma samples of patients with various cancers including ovarian and pancreatic cancers.[20,21]

Any biomarker candidates identified by genomic or proteomic approaches must be validated in a statistically sufficient number of cases and controls using a different quantitative method before being considered for clinical application.[22,23] Accordingly, we determined the relative plasma levels of Apo AI and C9 in 345 individuals using RPPM (Fig. 3) and confirmed the results in an independent cohort consisting of 378 plasma samples collected from healthy controls and patients with various diseases (Table 3). The collection and storage of all the plasma samples were performed under the same protocol to exclude any sampling biases. Conventionally, ELISA has been used for such validation, but the standard sandwich ELISA assay requires two antibodies that do not interfere with each other. As a result, the development of ELISA usually takes several months for every biomarker candidate protein. And more importantly, ELISA requires a relative large volume (~100 μL) of samples. Because the supply of clinical materials is often limited, it may be unfavorable to use hundreds of microliters of precise samples for preliminary experiments. Our high-density RPPM requires a minimal sample volume of the nanoliter order and one antibody. RPPM is an alternative validation method that can determine the
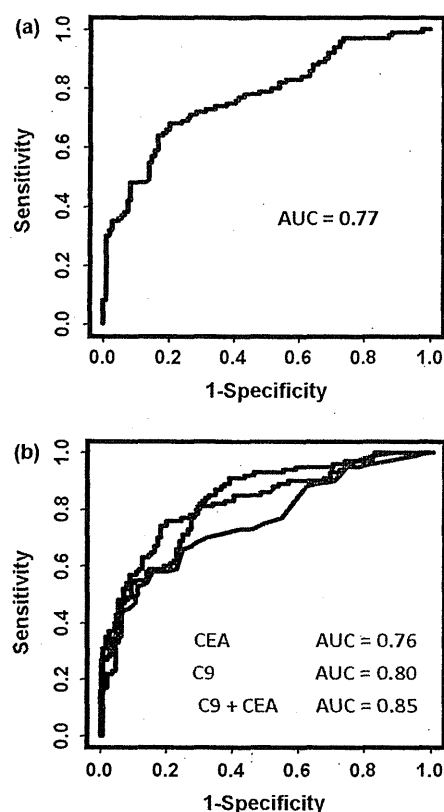
Fig. 4. Confirmation in an independent cohort. (a) Receiver operator characteristic (ROC) analysis of apolipoprotein AI (Apo AI; colorectal cancer patients [n = 100] over healthy controls [n = 109]). AUC, area under the curve. (b) ROC analysis of carcinoembryonic antigen (CEA), plasma complement component-9 (C9) and their combination (colorectal cancer patients [n = 100] over healthy controls [n = 109]).

clinical utility of candidate biomarker protein in a single experiment.[12]

Although protein microarray is a newly established technique and still requires improvement regarding validity and standardization,[24] it has been successfully used for analyzing clinical specimens of prostate cancer,[25] breast cancer,[26] rhabdomyosarcoma[27] and acute myeloid leukemia.[28,29] More recently, Grote et al.[30] used protein microarrays for the measurement of serum and plasma CA19-9. They printed a total of 149 sera and plasma samples obtained from pancreatic cancer patients, patients with chronic pancreatitis and healthy controls onto

nitrocellulose-coated slide glasses and obtained results comparable to conventional ELISA. They used 200-μm pins, and signals were detected using diaminobenzidine as a chromogen. We were able to spot as many as 6144 protein samples into a glass slide using a 100-μm innovative screw-shaped pin and hydrophobic surface technologies. The hydrophobic surface of microarrays mediates tight interaction with proteins and prevents protein spot diffusion.[16,17] Only with all these cutting-edge technologies was this level of high-density spotting of adhesive protein samples possible. Fluorescence immunostaining of our RPPM provided wide dynamic range and high reproducibility (Fig. 2). The linearity of fluorescence intensity was obtained in a wide range, and over 78% of quadruplicate showed a CV of < 0.1 (Fig. 2c). All these make our RPPM a reliable tool for biomarker validation.

The ninth component of complement (C9) is one of five component proteins (C5b, C6, C7, C8 and C9) of the membrane attack complex (MAC).[31] The MAC attaches to the surface of target cells and forms a pore across the cell membrane resulting in complement-dependent cytotoxicity (CDC). Aberrant activation of MAC has been implicated in the pathogenesis of various autoimmune and infectious diseases. We previously identified the significant increase of complement components C3 and C4A in the sera of endometrial cancer patients.[9] In the present study we found the plasma level of C9 was significantly elevated in colorectal cancer patients, including those with stage I and II diseases. The expression of membrane-bound CD46, CD55 and CD59 protects cancer cells from CDC,[32] but the precise role of complements and these modifiers in the process of carcinogenesis has not been fully established. Further efforts will be necessary to clarify the

biological significance of increased circulating C9 in patients with colorectal cancer.

In the present study we identified and validated C9 as a plasma biomarker potentially useful for the detection of early stage colorectal cancer using the combination of innovative proteomic technologies. Although the clinical significance of C9 must be clarified in an independent clinical study, we were able to demonstrate the utility of the combination of 2DICAL and RPPM in biomarker discovery and validation. The combination is a rapid approach that could be applicable to the discovery of biomarkers for any types of human malignancy.

Disclosure Statement

No potential conflict of interest relevant to this paper is declared.

References

1 Parkin DM, Bray F, Ferlay J, Pisani P. Global cancer statistics, 2002. *CA Cancer J Clin* 2005; **55**: 74–108.
2 Okuno K. Surgical treatment for digestive cancer. Current issues – colon cancer. *Dig Surg* 2007; **24**: 108–14.
3 Wakai K, Hirose K, Matsuo K *et al.* Dietary risk factors for colon and rectal cancers: a comparative case–control study. *J Epidemiol* 2006; **16**: 125–35.
4 Duffy MJ, van Dalen A, Haglund C *et al.* Tumour markers in colorectal cancer: European Group on Tumour Markers (EGTM) guidelines for clinical use. *Eur J Cancer* 2007; **43**: 1348–60.
5 Liotta LA, Petricoin EF. Serum peptidome for cancer detection: spinning biologic trash into diagnostic gold. *J Clin Invest* 2006; **116**: 26–30.
6 Omenn GS, States DJ, Adamski M *et al.* Overview of the HUPO Plasma Proteome Project: results from the pilot phase with 35 collaborating laboratories and multiple analytical groups, generating a core dataset of 3020 proteins and a publicly-available database. *Proteomics* 2005; **5**: 3226–45.
7 Honda K, Hayashida Y, Umaki T *et al.* Possible detection of pancreatic cancer by plasma protein profiling. *Cancer Res* 2005; **65**: 10613–22.
8 States DJ, Omenn GS, Blackwell TW *et al.* Challenges in deriving high-confidence protein identifications from data gathered by a HUPO plasma proteome collaborative study. *Nat Biotechnol* 2006; **24**: 333–8.
9 Negishi A, Ono M, Handa Y *et al.* Large-scale quantitative clinical proteomics by label-free liquid chromatography and mass spectrometry. *Cancer Sci* 2009; **100**: 514–9.
10 Ono M, Shitashige M, Honda K *et al.* Label-free quantitative proteomics using large peptide data sets generated by nanoflow liquid chromatography and mass spectrometry. *Mol Cell Proteomics* 2006; **5**: 1338–47.
11 Matsubara J, Ono M, Negishi A *et al.* Identification of a predictive biomarker for hematologic toxicities of gemcitabine. *J Clin Oncol* 2009; **27**: 2261–8.
12 Matsubara J, Ono M, Honda K *et al.* Survival prediction for pancreatic cancer patients receiving gemcitabine treatment. *Mol Cell Proteomics* 2010; **9**: 695–704.
13 Machida-Montani A, Sasazuki S, Inoue M *et al.* Atrophic gastritis, *Helicobacter pylori*, and colorectal cancer risk: a case-control study. *Helicobacter* 2007; **12**: 328–32.
14 Ono M, Matsubara J, Honda K *et al.* Prolyl 4-hydroxylation of α-fibrinogen: a novel protein modification revealed by plasma proteomics. *J Biol Chem* 2009; **284**: 29041–9.

15 Honda K, Yamada T, Hayashida Y *et al.* Actinin-4 increases cell motility and promotes lymph node metastasis of colorectal cancer. *Gastroenterology* 2005; **128**: 51–62.
16 Lee Y, Lee EK, Cho YW *et al.* ProteoChip: a highly sensitive protein microarray prepared by a novel method of protein immobilization for application of protein–protein interaction studies. *Proteomics* 2003; **3**: 2289–304.
17 Sasakura Y, Kanda K, Yoshimura-Suzuki T *et al.* Protein microarray system for detecting protein–protein interactions using an anti-His-tag antibody and fluorescence scanning: effects of the heme redox state on protein-protein interactions of heme-regulated phosphodiesterase from *Escherichia coli*. *Anal Chem* 2004; **76**: 6521–7.
18 Greene FL. TNM staging for malignancies of the digestive tract: 2003 changes and beyond. *Semin Surg Oncol* 2003; **21**: 23–9.
19 Breslow JL, Ross D, McPherson J *et al.* Isolation and characterization of cDNA clones for human apolipoprotein A-I. *Proc Natl Acad Sci U S A* 1982; **79**: 6861–5.
20 Zhang Z, Bast RC Jr, Yu Y *et al.* Three biomarkers identified from serum proteomic analysis for the detection of early stage ovarian cancer. *Cancer Res* 2004; **64**: 5882–90.
21 Kozak KR, Su F, Whitelegge JP, Faull K, Reddy S, Farias-Eisner R. Characterization of serum biomarkers for detection of early stage ovarian cancer. *Proteomics* 2005; **5**: 4589–96.
22 Ransohoff DF. Rules of evidence for cancer molecular-marker discovery and validation. *Nat Rev Cancer* 2004; **4**: 309–14.
23 Ludwig JA, Weinstein JN. Biomarkers in cancer staging, prognosis and treatment selection. *Nat Rev Cancer* 2005; **5**: 845–56.
24 Wulfkuhle JD, Edmiston KH, Liotta LA, Petricoin EF 3rd. Technology insight: pharmacoproteomics for cancer – promises of patient-tailored medicine using protein microarrays. *Nat Clin Pract Oncol* 2006; **3**: 256–68.
25 Grubb RL, Calvert VS, Wulkuhle JD *et al.* Signal pathway profiling of prostate cancer using reverse phase protein arrays. *Proteomics* 2003; **3**: 2142–6.
26 Rapkiewicz A, Espina V, Zujewski JA *et al.* The needle in the haystack: application of breast fine-needle aspirate samples to quantitative protein microarray technology. *Cancer* 2007; **111**: 173–84.
27 Petricoin EF 3rd, Espina V, Araujo RP *et al.* Phosphoprotein pathway mapping: Akt/mammalian target of rapamycin activation is negatively associated with childhood rhabdomyosarcoma survival. *Cancer Res* 2007; **67**: 3431–40.

28 Tibes R, Qiu Y, Lu Y *et al.* Reverse phase protein array: validation of a novel proteomic technology and utility for analysis of primary leukemia specimens and hematopoietic stem cells. *Mol Cancer Ther* 2006; **5**: 2512–21.

29 Kornblau SM, Tibes R, Qiu YH *et al.* Functional proteomic profiling of AML predicts response and survival. *Blood* 2009; **113**: 154–64.

30 Grote T, Siwak DR, Fritsche HA *et al.* Validation of reverse phase protein array for practical screening of potential biomarkers in serum and plasma:

accurate detection of CA19-9 levels in pancreatic cancer. *Proteomics* 2008; **8**: 3051–60.

31 Tschopp J, Podack ER, Muller-Eberhard HJ. Ultrastructure of the membrane attack complex of complement: detection of the tetramolecular C9-polymerizing complex C5b-8. *Proc Natl Acad Sci U S A* 1982; **79**: 7474–8.

32 Gorter A, Meri S. Immune evasion of tumor cells using membrane-bound complement regulatory proteins. *Immunol Today* 1999; **20**: 576–82.

Supporting Information

Additional Supporting Information may be found in the online version of this article:

Fig. S1. Verification of reverse-phase plasma microarray (RPPM).

Please note: Wiley-Blackwell are not responsible for the content or functionality of any supporting materials supplied by the authors. Any queries (other than missing material) should be directed to the corresponding author for the article.

Phase II study of erlotinib plus gemcitabine in Japanese patients with unresectable pancreatic cancer

Takuji Okusaka,[1,14] Junji Furuse,[2,3] Akihiro Funakoshi,[4] Tatsuya Ioka,[5] Kenji Yamao,[6] Shinichi Ohkawa,[7] Narikazu Boku,[8] Yoshito Komatsu,[9] Shoji Nakamori,[10] Haruo Iguchi,[11] Tetsuhide Ito,[12] Kazuhiko Nakagawa[13] and Kohei Nakachi[2]

[1]National Cancer Center Hospital, Tokyo; [2]National Cancer Center Hospital East, Kashiwa; [3]Kyorin University School of Medicine, Tokyo; [4]National Kyushu Cancer Center, Fukuoka; [5]Osaka Medical Center for Cancer and Cardiovascular Diseases, Osaka; [6]Aichi Cancer Center Hospital, Nagoya; [7]Kanagawa Cancer Center Hospital, Yokohama; [8]Shizuoka Cancer Center, Shizuoka; [9]Hokkaido University Hospital, Sapporo; [10]National Hospital Organization Osaka National Hospital, Osaka; [11]National Hospital Organization Shikoku Cancer Center, Ehime; [12]Kyushu University, Fukuoka; [13]Kinki University School of Medicine, Osaka, Japan

Erlotinib combined with gemcitabine has not been evaluated in Japanese patients with unresectable pancreatic cancer. This two-step phase II study assessed the safety and pharmacokinetics of erlotinib 100 mg/day (oral) plus gemcitabine 1000 mg/m² (i.v. days 1, 8, 15) in a 28-day cycle in the first step, and efficacy and safety in the second step. The primary end-point was safety. One hundred and seven patients were enrolled (first step, n = 6; second step, n = 101). The most common adverse event was RASH (compiled using the preferred terms rash, acne, exfoliative rash, dermatitis acneiform, erythema, eczema, dermatitis and pustular rash) in 93.4% of patients. One treatment-related death occurred. While interstitial lung disease-like events were reported in nine patients (8.5%; grade 1/2/3, 3.8/2.8/1.9%), all patients recovered or improved. The median overall survival, the 1-year survival rate and median progression-free survival were 9.23 months, 33.0% and 3.48 months, respectively. The overall response and disease control rates were 20.3% and 50.0%, respectively. In Japanese patients with unresectable pancreatic cancer, erlotinib plus gemcitabine had acceptable toxicity and efficacy that was not inferior to that seen in Western patients. (Cancer Sci 2011; 102: 425–431)

Approximately 232 000 individuals are diagnosed with pancreatic cancer worldwide each year, with an annual death rate estimated at 227 000.[1] In Japan, approximately 22 000 new cases were reported in 2005.[2] Furthermore, data from 2007 show that around 24 000 individuals in Japan died from pancreatic cancer, making this tumor type the fifth leading cause of cancer-related death.[3] The majority of pancreatic cancer cases are diagnosed at an unresectable stage when prognosis is extremely poor.

Current treatment for advanced pancreatic cancer is based on systemic chemotherapy with gemcitabine. Single-agent gemcitabine has been shown to extend median overall survival (OS) to 5.65 months in chemonaïve patients compared with 4.41 months in patients who received fluorouracil.[4] Addition of other cytotoxic agents to gemcitabine has not demonstrated survival benefits over gemcitabine alone.[5–13] The potential of combining gemcitabine with biological agents in patients with advanced pancreatic cancer has also been evaluated in several phase III studies, but these trials failed to show a survival benefit.[14–19]

Epidermal growth factor receptor (EGFR)-mediated signaling is associated with various cellular processes, and the dysregulation of these processes is common in tumorigenesis.[20,21] Furthermore, EGFR is overexpressed in many tumors and its overexpression is often associated with poor prognosis.[22–26] EGFR tyrosine-kinase inhibitors (TKI, such as erlotinib) are used in the treatment of various types of solid tumors.

Erlotinib has demonstrated antitumor activity in pancreatic cell lines[27] and was subsequently assessed as a potential therapeutic agent in pancreatic cancer. In the PA.3 study (n = 569), the risk of death with erlotinib plus gemcitabine was reduced by 18% versus gemcitabine alone (hazard ratio [HR], 0.82; 95% confidence interval [CI], 0.69–0.99; P = 0.038 after adjustment for stratification factors), with a median OS of 6.24 months vs 5.91 months, respectively. Erlotinib plus gemcitabine combination therapy provided significant improvements in the 1-year survival rate (23% vs 17%; P = 0.023) and progression-free survival (PFS; HR 0.77; 95% CI, 0.64–0.92; P = 0.004).[28] As a result, this combination was approved for use in pancreatic cancer in many countries.

In Japanese patients with non-small-cell lung cancer (NSCLC), a phase II study has specifically shown that erlotinib monotherapy is well tolerated and has promising antitumor activity.[29] However, there are no data on the use of erlotinib combined with gemcitabine in Japanese patients with pancreatic cancer. This phase II study evaluated the safety and efficacy of erlotinib in combination with gemcitabine in Japanese patients with unresectable locally advanced or metastatic pancreatic cancer.

Methods

Patients. Patients aged 20–80 years with histological/cytological evidence of unresectable locally advanced or metastatic adenocarcinoma/adenosquamous carcinoma of the pancreas were eligible for inclusion in the present study. Patients were required to have an Eastern Cooperative Oncology Group (ECOG) performance status (PS) of 0–2, adequate hematological, renal and hepatic function and a life expectancy of at least 2 months. No more than one prior regimen for pancreatic cancer was permitted. Patients who had received prior gemcitabine and/or a TKI were excluded from participation, as were those who had previously been exposed to a human epidermal growth factor receptor 2 (HER2) or EGFR inhibitor. Other key

exclusion criteria were: symptomatic cerebral metastases; a concurrent lung disorder (such as idiopathic pulmonary fibrosis, interstitial lung disease [ILD] or pneumoconiosis); concurrent or previous drug-induced pneumonia; or a history of radiation to the chest.

The study complied with the Declaration of Helsinki and Good Clinical Practice guidelines. Informed consent was obtained from all patients, and the protocol was approved by ethics committees at all participating institutions.

Study design and treatment. This was a phase II, multicentre, open-label, two-step study. In the first step, six patients were enrolled into the study and treated with oral erlotinib 100 mg/day on days 3–28, plus i.v. gemcitabine 1000 mg/m^2 on days 1, 8 and 15 in a 28-day cycle. The starting doses of erlotinib and gemcitabine were chosen in reference to the PA.3 study. Dose-limiting toxicities (DLT) were assessed in these study participants using the National Cancer Institute Common Terminology Criteria for Adverse Events v3.0 (NCI-CTCAE, National Cancer Institute, Bethesda, MD, USA). Dose-limiting toxicities were defined in conformity to the P1b study as follows:[30] (i) grade 4 decrease (i.e. to <500/mm^3) in neutrophil count >5 days; (ii) grade $\geq$3 decrease (i.e. to <1000/mm^3) in neutrophil count with associated fever ($\geq$38.5°C); (iii) grade 4 decrease in platelet count (i.e. to <25 000/mm^3); (iv) any grade ILD; (v) grade 4 elevation of alanine transaminase (ALT)/aspartate transaminase (AST) levels, or grade 3 elevation of ALT/AST levels >7 days; (vi) grade $\geq$3 non-hematological toxicity (excluding rash, hyperglycemia, γ-GTP and events that were judged to be transient/had no effect on study continuation); and (vii) dose-reduction/interruption required due to persistent adverse events (AE), which meant that the second cycle could not be started.

If treatment-related DLT occurred in no more than two of the six patients, transition to the second step of the study was permissible with approval of the Data Safety and Monitoring Committee (DSMC). If DLT occurred in three or more patients, transition to the second step was limited to those cases that were judged to be safe for this study after the DSMC had evaluated the safety data of the patients with a DLT. In the second step, it was planned that 94 patients would be treated with the same dose as the first step. Treatment was continued until disease progression, death, unacceptable toxicity or patient/investigator request.

The primary end-point of the study was safety, with secondary end-points including OS, 1-year survival rate, PFS, overall response rate (ORR), disease control rate (DCR = complete response [CR] + partial response [PR] + stable disease), pharmacokinetics (PK) and correlation of EGFR mutation status with outcomes.

Toxicity evaluation. Adverse events were monitored and graded using NCI-CTCAE v3.0. Clinical and laboratory assessments were conducted throughout the study. Adverse events prespecified in the study to be monitored carefully were rash, diarrhea, vomiting, liver dysfunction and ILD-like events. Chest X-ray examination to assess pulmonary toxicity was conducted weekly until week 4 and every 2 weeks thereafter. In addition, chest computed tomography (CT) scan was performed every 4 weeks. The DSMC reviewed the images and clinical data associated with all potential ILD-like events. All ILD-like events were reported to be serious AE (SAE), regardless of the grade.

Efficacy evaluation. The tumor response was assessed using Response Evaluation Criteria in Solid Tumors (RECIST) in patients who had at least one measurable target lesion. Tumors were measured using computed tomography (CT) at baseline and on day 22 of every two cycles thereafter. Median PFS, ORR and DCR were estimated by the extramural review. The relationship between efficacy and the severity of RASH (compiled

using the preferred terms rash, acne, exfoliative rash, dermatitis acneiform, erythema, eczema, dermatitis and pustular rash) was also examined.

Pharmacokinetic evaluation. Pharmacokinetic evaluation of erlotinib and its O-desmethylated metabolite (OSI-420) was performed in the six patients enrolled in the first step of the study. Venous blood samples were taken prior to erlotinib dosing on day 3 and day 8 of cycle 1 at 0.5, 1, 2, 4, 6, 8 and 24 h after erlotinib administration. Samples were also taken prior to gemcitabine infusion on days 1 and 8 at 0.5, 0.75, 1, 1.5, 2.5 and 4.5 h after dosing.

The plasma concentrations of erlotinib, OSI-420 and gemcitabine were measured by liquid chromatography, tandem mass spectrometry (LC-MS-MS). The LC-MS-MS analytical methods have been described previously.[31,32] Derived PK parameters included the maximum plasma drug concentration (C_{max}), time to C_{max} (t_{max}), area under the plasma drug concentration-time curve to the last plasma sample (AUC$_{last}$), terminal half-life ($t_{1/2}$) and oral clearance (Cl/F).

Biomarker analysis. EGFR mutations were assessed in patients with available tumor tissue specimens, which were formalin fixed and paraffin embedded. Samples were analyzed at a central laboratory where DNA was extracted and exons 18–21 sequenced using a nested PCR.

Statistical analysis. Progression-free survival and OS were estimated using the Kaplan–Meier method in all patients who received at least one dose of the study treatment, with 95% CI for the median duration calculated using Greenwood's formula. The Clopper–Pearson method was used to calculate the 95% CI around the ORR, DCR and AE rate. Multivariate analyses were performed for the occurrence of ILD-like events using the logistic regression model. Baseline characteristics investigated for this analysis included gender, age, lung metastasis, emphysema and various baseline laboratory values. The target enrollment was 100 patients, as this was required to evaluate the safety of erlotinib.

Results

Patient characteristics. Between December 2006 and October 2007, a total of 107 patients were enrolled (first step, n = 6; second step, n = 101) from 12 institutions (Fig. 1). One patient who enrolled into the second step did not receive treatment due to deterioration in PS prior to the start of treatment. A total of 106 patients were evaluable for safety (safety population, full analysis set).

The patient demographics and baseline characteristics are shown in Table 1. The median age was 62 years (range, 36–78) and 52.8% of patients were male. Almost all patients were chemonaïve (95.3%). The majority (75.5%) of patients had an ECOG PS of 0 and most (83.0%) had metastatic disease. Over half (63.2%) of the patients had a history of current or past smoking.

Toxicity and dose modifications. The median duration of erlotinib exposure was 102.5 days and its median dose intensity was 100.0 mg/day, with the majority of patients (78.3%) receiving more than 90% of the relative dose intensity. The median duration of gemcitabine treatment was 4.0 cycles and its median dose intensity was 688.0 mg/m^2 per week, with approximately half of the patients (51.4%) receiving more than 90% of the relative dose intensity.

As only one patient had a DLT (grade 3 diarrhea) in the first step, the second step of the study was initiated. One hundred and six patients received at least one dose of erlotinib; these patients were assessable for toxicity. Treatment-related AE and treatment-related changes in laboratory values are summarized in Table 2; most of these were mild to moderate in severity. The most frequently reported AE was RASH, which occurred in